Propagation and Ghosts in the Classical Kagome Antiferromagnet

J. Robert,[1] B. Canals,[2] V. Simonet,[2] and R. Ballou[2]
[1]*Laboratoire Léon Brillouin, CEA-CNRS, CEA-Saclay, 91191 Gif-sur-Yvette, France*
[2]*Institut NEEL, CNRS & Université Joseph Fourier, BP 166, 38042 Grenoble Cedex 9, France*
(Received 9 July 2008; published 12 September 2008)

We investigate the classical spin dynamics of the kagome antiferromagnet by combining Monte Carlo and spin dynamics simulations. We show that this model has two distinct low temperature dynamical regimes, both sustaining propagative modes. The expected gauge invariance type of the low energy, low temperature, out-of-plane excitations is also evidenced in the nonlinear regime. A detailed analysis of the excitations allows us to identify ghosts in the dynamical structure factor, i.e., propagating excitations with a strongly reduced spectral weight. We argue that these dynamical extinction rules are of geometrical origin.

DOI: 10.1103/PhysRevLett.101.117207 PACS numbers: 75.10.Hk, 75.40.Gb, 75.40.Mg, 75.50.Ee

Geometrical frustrated magnets are currently a source of high interest for the exotic phases and unexpected dynamics that they are liable to generate. Full insight into their behavior is still far from being acquired, especially at the lowest temperatures.

A prototype is the classical Heisenberg kagome antiferromagnet [1]. As a basic distinctive feature of the geometrical frustration, its ground state consists of a continuous connected manifold of spin configurations. At high temperatures ($T/J \gtrsim 0.1$, with J the first neighbor exchange), the system is paramagnetic. It enters what we shall call from now on a cooperative paramagnetic phase in the range $5 \times 10^{-3} \lesssim T/J \lesssim 0.1$ where short range correlations are enhanced. At the lowest temperatures ($T/J \lesssim 5 \times 10^{-3}$), thermal fluctuations above each of the spin configurations of the ground state manifold are not equivalent and drive an entropic based order out of disorder mechanism [2], eventually selecting a spin plane [3] and developing an octupolar order [4]. We shall call this phase coplanar to distinguish it from the former. While in both low temperature regimes it was shown that spin-pair correlations remain short ranged [5], it is only in the coplanar phase that the continuous degeneracy of the manifold was argued to be reduced to a discrete one, described by the three colorings of the lattice [6]. Altogether, these results provide a rather clear picture of the thermodynamics of the classical kagome antiferromagnet, which should apply to experimental compounds with large magnetic moments but also be of some relevance for low spin systems, since quantum fluctuations often play a significant role at very low temperatures only.

A much poorer understanding of the spin dynamics is in contrast available. To our knowledge, only one numerical investigation has so far been conducted [7], which furthermore was not resolved in momentum vectors $\mathbf{Q}$, thus ignoring any diffusive or propagating aspects of the excitations. In this Letter, we analyze the temperature dependent dynamics of the classical kagome antiferromagnet from two points of views. We first show that at low temperatures, spin waves (SW) do propagate and are sensitive to the underlying spin texture, either cooperative paramagnetic or coplanar. Quantitative analysis of the dynamical structure factor is performed and provides the characteristic time scales. Additionally, the invariance of the linear SW spectra with respect to the ground state spin configurations on which they are built is evidenced in a wide range of temperatures, including those where nonlinear effects are at play. We next put forward that peculiar excitations develop that would be almost invisible to dynamical spin-pair correlations sensitive probes, such as inelastic neutron scattering.

The numerical method used in this Letter is a combination of a hybrid Monte Carlo (MC) method, which allows generating samples of spin arrays at a given temperature, and an integration of the nonlinear coupled equations of motion for spin dynamics (SD):

$$\frac{d\mathbf{S}_i}{dt} = J\left(\sum_j \mathbf{S}_j\right) \times \mathbf{S}_i, \tag{1}$$

where j is a first neighbor of i and $J > 0$ is the antiferromagnetic exchange [8]. The numerical integration has been performed up to $t = 1000J^{-1}$ using an 8th-order Runge-Kutta (RK) method with an adaptative step-size control. The RK error parameter as well as the RK order have been fixed in order to preserve the Euclidean distance with a test-full diffusion of Eq. (1) performed with the more robust but time consuming Burlisch-Stoer algorithm. As a result, trivial constants of motion, such as the total energy E_{tot} and magnetization M_{tot}, are conserved with a relative error smaller than 10^{-6}. As for the spin arrays samplings by the MC method, a first run has been performed in order to find an optimal set of temperatures for a parallel tempering scheme [9], which minimizes the ergodic time [10]. A reduction of the solid angle for each spin flip trial together with rotations around the local molecular fields ensure a rate acceptance above 40%. The numerical simulations

reported in this Letter were performed on samples of $L \times L \times 3$ spins with $L = 36$ and periodic boundary conditions. Our interest lies in the scattering function, namely, the time and space Fourier transform of the dynamical spin-pair correlations:

$$S(\mathbf{Q}, \omega) = \sum_{ij} \int \frac{dt}{\sqrt{2\pi N}} \langle \mathbf{S}_i(0) \cdot \mathbf{S}_j(t) \rangle e^{-i\mathbf{Q}\cdot\mathbf{R}_{ij}} e^{-i\omega t} \quad (2)$$

where $\mathbf{Q}$ and ω are the momentum vector and energy transfer, $\langle \ldots \rangle$ is the ensemble average, and $\mathbf{R}_{ij} = \mathbf{R}_j - \mathbf{R}_i$ and N are the number of spins.

Details about static properties will not be given here. It is worth noting, however, that our results for $\omega = 0$ at very low temperatures ($T/J \lesssim 5 \times 10^{-3}$), when entropic selection is at work, points towards fluctuations predominantly associated with the so-called $q = \sqrt{3} \times \sqrt{3}$ phase. This meets with previous conclusions, although those were inferred from instantaneous ensemble averages [5,6,11]. We similarly got very good agreement with previous numerical or analytical investigations of specific heat, coplanar ordering, or the instantaneous scattering function [3–5,12], giving confidence on the quality of our numerical simulations.

Let us now focus on the dynamical properties of the kagome antiferromagnet. Although the propagation of collective excitations may appear unexpected in such a system, where the spin-pair correlation function decays exponentially with distance at finite temperatures [5], a sufficient temporal and spatial stiffness may lead to the propagation of SW in locally ordered regions. Therefore, a required condition for the development of SW excitations is an increase with decreasing temperature of the autocorrelation time τ_a featuring the lifetime of locally ordered states. τ_a has been numerically evaluated by integrating the scattering function over all $\mathbf{Q}$ values in the reciprocal space, which gives access to the time Fourier transform of the autocorrelation function $A(t) = \langle \mathbf{S}_i(0) \cdot \mathbf{S}_i(t) \rangle$. A fit of the obtained quasielastic (QE) signal using a Lorentzian shape $\frac{I_0 \Gamma_a}{\Gamma_a^2 + \omega^2}$, associated with a decaying exponential law $A(t) = \exp(-\Gamma_a t)$ in time space, allows extracting the half width at half maximum (HWHM) $\Gamma_a \propto 1/\tau_a$. As the temperature is decreased, this shows an algebraic variation $\Gamma_a = \mathcal{A} T^{\zeta}$ with $\zeta = 0.995 \pm 0.018$ for $T/J \lesssim 0.1$ [see Fig. 3(a)], transposing to a slowing down of the spin fluctuations, but nevertheless no spin freezing even at temperatures as low as $T/J = 5 \times 10^{-4}$. Interestingly, the same thermal variation is observed in the cooperative paramagnetic ($T/J \gtrsim 5 \times 10^{-3}$) and the coplanar states ($T/J \lesssim 5 \times 10^{-3}$) regimes, asserting that the entropic selection favoring the coplanar manifold has no influence on the lifetime τ_a of locally ordered states. Now that we have characterized the temporal stiffness associated with the T^{-1} slowing down of τ_a, we address the question of well-defined excitations as well as their possible propagation. Evidence of the existence of SW-type excitations at low temperatures is explicit in the excitation spectrum for $T/J = 5 \times 10^{-4}$ (see Fig. 1). For comparison, the linear spin wave (LSW) spectrum [11] emerging from the pure $q = \sqrt{3} \times \sqrt{3}$ phase is shown. The SD simulations evidence a large weight of $S(\mathbf{Q}, \omega)$ at this LSW spectrum, confirming that the $q = \sqrt{3} \times \sqrt{3}$ short range dynamical correlations are favored at very low temperature.

The analysis of the spectrum as a function of the temperature allows more insight into the formation of SW excitations. We show in Fig. 2 the frequency dependence of $S(\mathbf{Q}, \omega)$ at the point $\mathbf{Q}_0 = 2\pi(3/4, 0)$ in the reciprocal space, located between the Brillouin zone (BZ) boundary and the BZ center (see Fig. 1), where the soft, acoustic, and optical modes are particularly easy to distinguish. These constant-$\mathbf{Q}$ scans are represented for temperatures from $T/J = 0.5$ to 5×10^{-4}. At high temperatures ($T/J \gtrsim 0.2$), only a QE signal centered at $\omega = 0$ contributes to the scattering function $S(\mathbf{Q}, \omega)$. A single broad excitation at finite energy comes into sight on decreasing T/J from 0.2 to 10^{-2}, although strongly softened compared with the LSW theory expectation (see inset of Fig. 2). Below $T/J = 10^{-2}$, the broad peak splits into two excitations, respectively, associated with SW acoustic modes and emerging soft modes, gradually separating from each other and getting thinner as the temperature goes down (see Fig. 2). The softening of the modes dies away to disappear below $T/J = 5 \times 10^{-4}$. The soft mode, expected to be nondispersive in LSW theory, is here observed at finite energy, due to the nonlinear nature of Eq. (1), which takes account of the interactions between the SW. This effect is expected to decrease with temperature, which is consistent with the fact that the soft mode drops to zero energy when temperature goes down (inset of Fig. 2). Finally, one can discern an additional peak at $\omega \simeq 2J$ for $T/J < 5 \times 10^{-3}$, corresponding to optical modes.

Each mode i of the excitation spectrum can be characterized by its dispersion relation $\omega^i(\mathbf{Q})$, its lifetime $\tau^i_{\mathrm{SW}} \propto (\Gamma^i_{\mathrm{SW}})^{-1}$, and its intensity I^i_0, all these quantities being

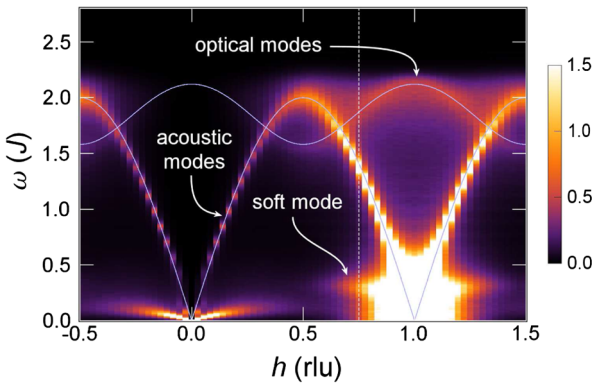

FIG. 1 (color online). Intensity map (arb. units) of the scattering function vs ω and $\mathbf{Q} = (h, 0)$, for $T/J = 5 \times 10^{-4}$. The LSW dispersion relations $\omega(\mathbf{Q})$ for the phase $q = \sqrt{3} \times \sqrt{3}$ are plotted as blue lines. The white dotted line corresponds to the constant-$\mathbf{Q}$ scans presented on Fig. 2.

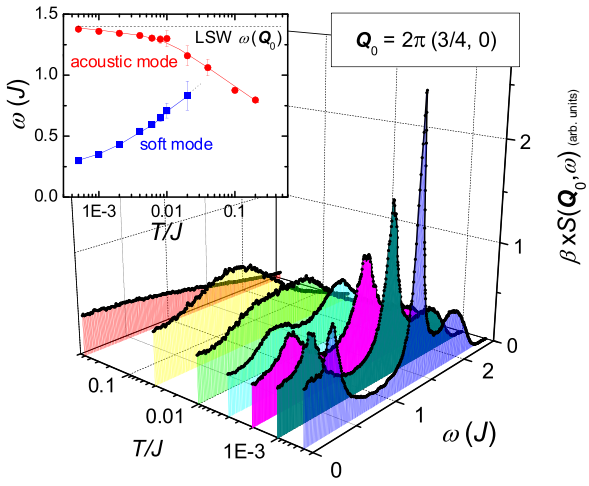

FIG. 2 (color online). Temperature weighted scattering function vs energy at different temperatures for $\mathbf{Q}_0 = 2\pi(3/4, 0)$. Inset: position of soft and acoustic modes vs temperature; error bars obtained from several fitting processes.

accessible by fitting the excitation spectrum at different temperatures and $\mathbf{Q}_0$ values. Assuming Lorentzian shape for magnetic excitations, the scattering function writes

$$S(\mathbf{Q}_0, \omega) = \sum_i \frac{I_0^i \Gamma^i}{(\Gamma^i)^2 + (\omega \pm \omega^i(\mathbf{Q}_0))^2} \qquad (3)$$

where i runs over soft, acoustic, and optical magnetic peaks for a particular $\mathbf{Q}_0$ value. We show in Fig. 3(b) the thermal variation of the resulting SW HWHM $\Gamma_{\mathrm{SW}} \propto \tau_{\mathrm{SW}}^{-1}$ for $\mathbf{Q}_0 = 2\pi(3/4, 0)$. It is found out, contrarily to τ_a [see Fig. 3(a)], that τ_{SW} follows two distinct regimes below and above $T/J = 5 \times 10^{-3}$, both consistent with an algebraic law $\tau_{\mathrm{SW}} = \mathcal{A} T^{-\zeta}$. τ_{SW} is in principle reduced by two physical processes. The first, common to all magnetic systems, is associated with the thermal fluctuations and anharmonic interactions between SW modes. In a disordered medium, this process is overwhelmed by a second one, induced by the motion of the system between the different ground states. In other words, even in the linear approximation, one is left with a set of linear equations of motions with time dependent initial conditions, the time variations of those being set by the autocorrelation time τ_a. In the pyrochlore antiferromagnet, it has been shown that τ_a is also proportional to T^{-1} and based on the above interpretation, it was proposed that the SW lifetime τ_{SW} is proportional to $T^{-1/2}$ [13]. This behavior is expected at least in the cooperative paramagnetic regime. In the corresponding temperature range, we find $\zeta = 0.18 \pm 0.07$, which is much lower than $\frac{1}{2}$. In the low T regime, due to the selection of coplanar spin configurations, the out-of-plane $\omega^{\perp}(\mathbf{Q})$ and the in-plane $\omega^{\parallel}(\mathbf{Q})$ modes become different, which allows distinguishing the corresponding scattering process $S(\mathbf{Q}, \omega) = S^{\perp}(\mathbf{Q}, \omega) + S^{\parallel}(\mathbf{Q}, \omega)$. Within the LSW, or equivalently at very low temperatures, the

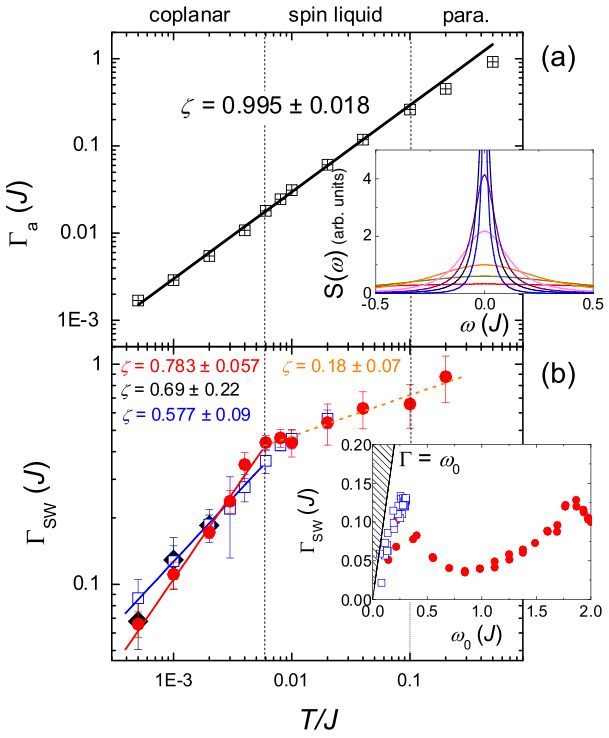

FIG. 3 (color online). (a) $\Gamma_a \propto \tau_a^{-1}$ obtained by fitting the QE signal $S(\omega)$, shown in the inset at several temperatures from $T/J = 0.5$ to 5×10^{-4}. (b) $\Gamma_{\mathrm{SW}} \propto \tau_{\mathrm{SW}}^{-1}$ for the soft (blue squares), in-plane (black diamonds) and out-of-plane (red circles) acoustic modes for $\mathbf{Q}_0 = 2\pi(3/4, 0)$. The error bars have been obtained by averaging over different fitting processes. If not seen, they are smaller than the symbols. The inset displays Γ_{SW} as a function $\omega_0 = \omega(\mathbf{Q})$, i.e., for several $\mathbf{Q}$ values. The hatched region forbids propagating excitations.

out-of-plane scattering function $S^{\perp}(\mathbf{Q}, \omega)$ is gauge invariant–like, i.e., it does not depend on the three coloring state on top of which the excitations develop [see Fig. 4(b), left]. Conversely, the in-plane contribution $S^{\parallel}(\mathbf{Q}, \omega)$ differs for each configuration it is build on [see Fig. 4(b), right]. In this coplanar regime, τ_{SW} seems to behave in similar ways for in-plane ($\zeta = 0.69 \pm 0.22$) and out-of-plane ($\zeta = 0.783 \pm 0.057$) acoustic modes, whereas ζ is slightly weaker for the soft mode ($\zeta = 0.577 \pm 0.09$). Thereby, we clearly see two distinct dynamical regimes with a ζ value in the coplanar phase significantly larger than the value in the cooperative paramagnetic phase. This suggests that the SW lifetime is sensitive to the entropic selection of the coplanar manifold, that latter inducing some kind of stiffness in the spin texture. We can also wonder about the propagation of these magnetic excitations. If $\Gamma_{\mathrm{SW}}/\omega_0 < 1$ for a given mode, it can be considered as a propagative SW, its lifetime τ_{SW} being longer than its period ω_0^{-1}. This actually is the case for the soft and acoustic modes, at least up to $T/J \lesssim 0.1$ (see inset of Fig. 3(b) for $T/J = 5 \times 10^{-4}$). This underlines that SW propagation in the kagome antiferromagnet,

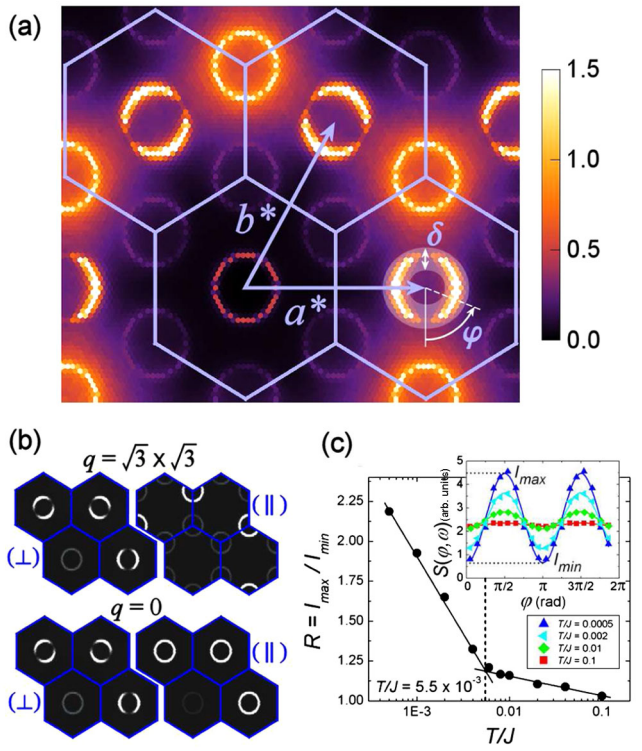

FIG. 4 (color online). (a) Intensity map (arb. units) in reciprocal space for $\omega = J$ and $T/J = 5 \times 10^{-4}$. The first and neighboring BZ are in blue (or gray). (b) Out-of-plane ($\perp$) (left) and in-plane ($\parallel$) (right) components for $q = \sqrt{3} \times \sqrt{3}$ and $q = 0$ spin configurations. (c) Anisotropy parameter $R = I_{\max}/I_{\min}$ vs temperature. Inset: scattering function plotted for different temperatures in the function of φ, as defined in (a).

although of a different nature, is possible in both regimes of cooperative paramagnetism and entropy induced coplanarity.

We finally focus on the spectral weight distribution in reciprocal space, which is nonuniform for the excitations emerging from the BZ centers, i.e., the out-of-plane acousticlike modes. A two-dimensional intensity map in reciprocal space is shown in Fig. 4(a), for $\omega = J$ and $T/J = 5 \times 10^{-4}$. The spectral weight $S(\mathbf{Q}, J)$ reaches its maximum value $I_{\max}$ along the $\mathbf{a}^\star$, $\mathbf{b}^\star$, or $\mathbf{a}^\star - \mathbf{b}^\star$ axis, and fades out in each corresponding perpendicular direction (with an intensity $I_{\min}$). This results in the presence of "ghosts" in the excitation rings, i.e., existing excitations with a strongly reduced cross section, that would be invisible, e.g., in neutron scattering experiments. Parametrizing these rings by the angle φ and integrating over a small width δ of the ring [see Fig. 4(a)] allows us to quantitatively analyze the spectral weight anisotropy as a function of the temperature. Figure 4(c) displays the evolution of the anisotropy parameter $R = I_{\max}/I_{\min}$ with the temperature. Strong discrepancies between the cooperative paramagnetic regime ($R \simeq 1$) and the entropy driven coplanar regime, in which the anisotropy strongly increases with decreasing temperature, are evidenced. At the lowest temperatures, where SW propagates onto a disordered manifold, the strongly fluctuating spin texture could therefore be expected to drive these extinctions. Actually, two distinct arguments rather support a purely geometrical origin. First, out-of-plane excitations are gauge invariant–like. Therefore, the fluctuating nature of the manifold should not play any role. Second, we have numerically computed $S(\mathbf{Q}, \omega)$ for configurations prepared in slightly distorted ordered $q = 0$ and $q = \sqrt{3} \times \sqrt{3}$ phases and performed a LSW expansion around these two phases [Fig. 4(b)]. All calculations reproduce this spectral anisotropy, pointing out that the ghost excitations rather originate from the peculiar geometry of the lattice revealed by spin coplanarity.

In conclusion, the propagation of spatially structured collective excitations has been numerically evidenced and quantitatively studied in the classical kagome antiferromagnet. Although the SW exist in both cooperative paramagnetic and coplanar regimes, their lifetime was found very sensitive to the entropic selection occurring below $T/J = 5 \times 10^{-3}$, in contrast with the same inverse temperature dependence of the autocorrelation time in both regimes. At very low temperatures, these propagative modes possess a noteworthy nonuniform spectral weight expressing effective dynamical extinction rules.

We would like to thank C. Henley and E. Bonet for helpful discussions. B. C. also thanks Shan-Ho Tsai for a useful correspondence at the early stages of this work.

[1] C. Zeng and V. Elser, Phys. Rev. B **42**, 8436 (1990); C. Zeng and V. Elser, Phys. Rev. B **51**, 8318 (1995).
[2] J. Villain, Z. Phys. B **33**, 31 (1979).
[3] J. T. Chalker, P. C. W. Holdsworth, and E. F. Shender, Phys. Rev. Lett. **68**, 855 (1992).
[4] M. Zhitomirsky, arXiv:0805.0676v1.
[5] J. N. Reimers and A. J. Berlinsky, Phys. Rev. B **48**, 9539 (1993).
[6] D. A. Huse and A. D. Rutenberg, Phys. Rev. B **45**, 7536 (1992).
[7] A. Keren, Phys. Rev. Lett. **72**, 3254 (1994).
[8] S.-H. Tsai, A. Bunker, and D. P. Landau, Phys. Rev. B **61**, 333 (2000).
[9] K. Hukushima and K. Nemoto, J. Phys. Soc. Jpn. **65**, 1604 (1996).
[10] H. G Katzgraber, S. Trebst, D. A Huse, and M. Troyer, J. Stat. Mech. (2006) P03018.
[11] A. B. Harris, C. Kallin, and A. J. Berlinsky, Phys. Rev. B **45**, 2899 (1992).
[12] D. A. Garanin and B. Canals, Phys. Rev. B **59**, 443 (1999).
[13] R. Moessner and J. T. Chalker, Phys. Rev. Lett. **80**, 2929 (1998); Phys. Rev. B **58**, 12049 (1998).